Supporting Information for

Construction of Bicontinuous Donor-acceptor Hybrid Material at the Molecular Level by Inserting Inorganic Nanowires into Porous MOFs

Jian-Jun Liu, Ying-Fang Guan, Ling Li, Yong Chen, Wen-Xin Dai, Chang-Cang Huang and Mei-Jin Lin**

Jian-Jun Liu, Ying-Fang Guan, Ling Li, Dr. Yong Chen, Prof. Wen-Xin Dai, Prof. Chang-Cang Huang and Prof. Mei-Jin Lin*

State Key Laboratory of Photocatalysis on Energy and Environment, College of Chemistry, Fuzhou University

Fuzhou, 350116, P.R. China. E-mail: meijin_lin@fzu.edu.cn (Prof. LIN), cchuang@fzu.edu.cn (Prof. HUANG)

Table of Contents:

1. Experimental Details and Synthesis

Materials and methods: All reagents were purchased commercially and used without further purification. The organic ligand *N*, *N*′-bis(carboxyethyl)-4,4'-bipyridinium (BCEbpy) was synthesized following the reported process [S1]. Elemental analyses of C, H, and N were performed on an Elementar Vario EL III microanalyzer. IR spectra were recorded in the range 4000-400 cm^{-1} on a Perkin-Elmer FT-IR spectrum 2000 spectrometer with pressed KBr pellets. Powder X-ray diffraction (PXRD) patterns were recorded with a Rigaku MiniFlex-II X-Ray diffractometer with Cu Kα radiation (λ = 1.54178 Å). TGA measurements were performed on a TG-209 system with a heating rate of 10 °C/min under an N_2 and air atmosphere. UV-Vis diffuse reflectance spectra were recorded at room temperature on a Varian Cary 500 UV-Vis spectrophotometer equipped with an integrating sphere. The single crystal electrodes were made using silver plastic and 100 μm gold line by placing the crystal between two electrodes. And the temperature-dependent and light-dependent I-V curve measurements have been performed on Keithley 4200 semiconductor characterization system (Keithley, Cleveland, OH, USA) equipped with a solar simulator (Sun 2000, Abet Technologies, Milford, CT, USA).

Synthesis of $[K_5Zn_2(BCEbpy)_3(OH)_2(H_2O)_2]_n \cdot [Pb_6I_{19}]_n$ (1): A solution of $Zn(CH_3COO)_2 \cdot 2H_2O$ (0.4 mmol, 87.8 mg in 5 mL of methanol) was carefully layered on a saturated KI solution (5 mL) containing PbI_2 (0.1 mmol, 46.1 mg) and BCEbpy (0.2 mmol, 54.4 mg) with MeOH/H_2O (1 mL/1 mL) placed between the two layers. Dark red platelike crystals of **1** formed in a few days. The product was collected by filtration and dried in the vacuum oven. Yield: 45% based on PbI_2. Elemental Analysis (%): Calcd: C 10.36, N 1.72, H 0.86; Found: C 10.45, N 1.74, H 0.93.

Synthesis of $[ZnI_2(BCEbpy)]$ (2): The organic BCEbpy (0.2 mmol, 54.4 mg) was completely dissolved in a mixed solution of water/DMF (4 mL: 1 mL) under stirring. The pH of the mixed solution was adjusted to ca. 7.0 by adding 0.1 M aqueous NaOH dropwise. And then, 1 mL of ZnI_2 (0.2 mmol, 64.0 mg) solution was added to the above solution. After the mixture was further stirred for 5 min, the residue was filtered. Reddish brown crystals were obtained after the filtrate was allowed to stand for 3 days.

Conductivity measurements： We chose a single crystal that was a uniform rectangle shape on the optical microscope, and placed the crystal onto a piece of glass slide. The conductive silver paste was used to fix the two ends of a single crystal, which were further connected with two gold lines (0.1mm). The two gold lines at the periphery of the crystal covered the whole rectangle faces to ensure unidirectional conduction. When all the silver paste was completely dry after about 2 h, this device was put on a thermostatic stage (solar simulator for photoconductivity

measurement), and the conductivity along the fixed direction was measured by using Keithley 4200 semiconductor characterization system(Scheme S1 and Figure S15). The size of the crystal 1 was measured by a calibrated low-resolution optical microscope (Lycra). In the case of 1, three single crystals were selected out to measure, and the final data were the average of the records. For 2, only one crystal was chosen because the texture is so fragile that makes it difficult to measure its conductivity.

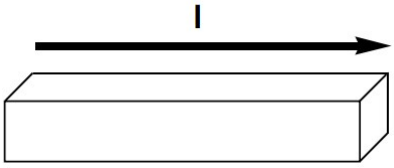

Scheme S1. The flowing directions of current in single crystals of **1** and **2**.

2. X-ray single-crystal diffraction analysis

2.1 Methods and crystal data

Suitable single crystal of hybrid **1** and **2** was mounted on glass fiber for the X-ray measurement. Diffraction data were collected on a Rigaku-AFC7 equipped with a Rigaku Saturn CCD area-detector system. The measurement was made by using graphic monochromatic Mo Kα radiation (λ = 0.71073 Å) at 153 K under a cold nitrogen stream. The frame data were integrated and absorption correction using a Rigaku *CrystalClear* program package. All calculations were performed with the *SHELXTL-97* program package [S2], and structures were solved by direct methods and refined by full-matrix least-squares against F^2. All non-hydrogen atoms were refined anisotropically, and hydrogen atoms of the organic ligands were generated theoretically onto the specific atoms except for the water molecules. Crystallographic data have been deposited with the Cambridge Crystallographic Data Center (CCDC) as supplementary publication number CCDC 1509713 and 1517893 for **1** and **2**, respectively, which can be obtained free of charge from CCDC *via* www.ccdc.cam.ac.uk/data_request/cif.

Table S1. Crystal Data and Structure Refinements for **1** and **2**

Complex	**1**	**2**
Empirical Formula	$C_{42}H_{36}I_{19}K_5N_6O_{16}Pb_6Zn_2$	$C_{14}H_{12}IN_2O_4Zn_{0.5}$
Color and habit	Dark red plate	Reddish
Formula weight	4861.25	431.84
Crystal system	Triclinic	Monoclinic
Space group	$P\bar{1}$	$P2/n$

a (Å)	12.038(2)	18.7223(11)
b (Å)	12.491(3)	5.7758(4)
c (Å)	16.889(3)	20.8283(14)
α (deg)	93.07(3)	90
β (deg)	103.47(3)	91.165(6)
γ (deg)	90.98(3)	90
V (Å^3)	2465.0(8)	2251.8(3)
Z	1	4
T (K)	153(2)	153(2)
ρ_{calc}(g/cm^3)	3.275	1.274
μ (Mo Kα) (mm^{-1})	16.892	1.954
F(000)	2112	840
Collected reflections	24246	14848
Unique reflections	11048(0.0384)	3825 (0.0422)
No. of observations	8256	3152
GOF	1.053	1.187
R_1,wR_2 (I>2σ(I))	0.0622, 0.1731	0.1313, 0.4515
R_1,wR_2 (all data)	0.0847, 0.1905	0.1455, 0.4748

Table S2. Selected bond lengths (Å) and bond angles (°) for **1**

Bond	Distance	Bond	Distance
Zn(1)-O(13)	1.84(3)	Zn(1)-O(1)	1.974(12)
Zn(1)-O(4)#1	2.137(19)	Zn(1)-I(1)	2.539(6)
I(1)-K(2)#2	3.595(6)	I(1)-K(1)	3.754(7)
I(2)-Pb(2)	3.0438(16)	I(2)-K(1)	3.609(6)
I(3)-Pb(2)	3.1216(18)	I(3)-Pb(3)#3	3.2536(18)
I(4)-Pb(2)	3.1288(17)	I(4)-Pb(3)#4	3.1704(15)
I(5)-Pb(1)	3.1067(15)	I(5)-Pb(2)	3.3846(18)
I(5)-K(2)#5	3.687(5)	I(6)-Pb(1)	3.1853(17)
I(6)-Pb(2)	3.3450(15)	I(7)-Pb(3)	3.1988(15)
I(7)-Pb(1)	3.2620(17)	I(8)-Pb(1)	3.0478(17)
I(8)-K(1)	3.734(5)	I(9)-Pb(3)#6	3.3344(15)
I(9)-Pb(2)#4	3.3961(16)	I(9)-Pb(1)	3.4077(14)

I(9)-Pb(3)	3.4239(17)	I(10)-Pb(3)	3.0187(17)
I(10)-K(2)#7	3.504(5)		
Angle	(°)	Angle	(°)
O(13)-Zn(1)-O(1)	105.4(11)	O(13)-Zn(1)-O(4)#1	96.1(12)
O(1)-Zn(1)-O(4)#1	109.6(6)	O(13)-Zn(1)-I(1)	117.0(12)
O(1)-Zn(1)-I(1)	120.2(5)	O(4)#1-Zn(1)-I(1)	105.8(6)
Zn(1)-I(1)-K(2)#2	112.49(15)	Zn(1)-I(1)-K(1)	107.31(16)
K(2)#2-I(1)-K(1)	74.88(13)	Pb(2)-I(2)-K(1)	103.20(10)
Pb(2)-I(3)-Pb(3)#3	97.55(5)	Pb(2)-I(4)-Pb(3)#4	99.32(4)
Pb(1)-I(5)-Pb(2)	91.23(4)	Pb(1)-I(5)-K(2)#5	160.66(9)
Pb(2)-I(5)-K(2)#5	105.45(9)	Pb(1)-I(6)-Pb(2)	90.60(4)
Pb(3)-I(7)-Pb(1)	93.47(4)	Pb(1)-I(8)-K(1)	107.34(10)
Pb(3)#6-I(9)-Pb(2)#4	90.88(4)	Pb(3)#6-I(9)-Pb(1)	168.40(3)
Pb(2)#4-I(9)-Pb(1)	100.16(4)	Pb(3)#6-I(9)-Pb(3)	96.67(4)
Pb(2)#4-I(9)-Pb(3)	89.50(4)	Pb(1)-I(9)-Pb(3)	87.05(4)
Pb(3)-I(10)-K(2)#7	106.27(10)		

Symmetry transformations used to generate equivalent atoms: #1-x+2, -y+1, -z+1; #2 -x+2, -y+1, -z; #3 x+1, y, z; #4 -x+2, -y, -z+1; #5 x, y-1, z; #6 -x+1, -y, -z+1; #7 x-1, y-1, z.

Table S4. Selected bond lengths (Å) and bond angles (°) for **2**

Bond	Dist.	Bond	Dist.
Zn(1)-O(1)	1.957(6)	Zn(1)-O(3)	1.969(6)
Angle	(°)	Angle	(°)
O(1)-Zn(1)-O(1)#1	99.2(4)	O(1)-Zn(1)-O(3)	112.4(3)
O(1)#1-Zn(1)-O(3)	115.4(3)	O(3)-Zn(1)-O(3)#1	102.7(4)

Symmetry transformations used to generate equivalent atoms: #1 -x+3/2, y, -z+1/2.

2.2 Some important views of 1 and 2

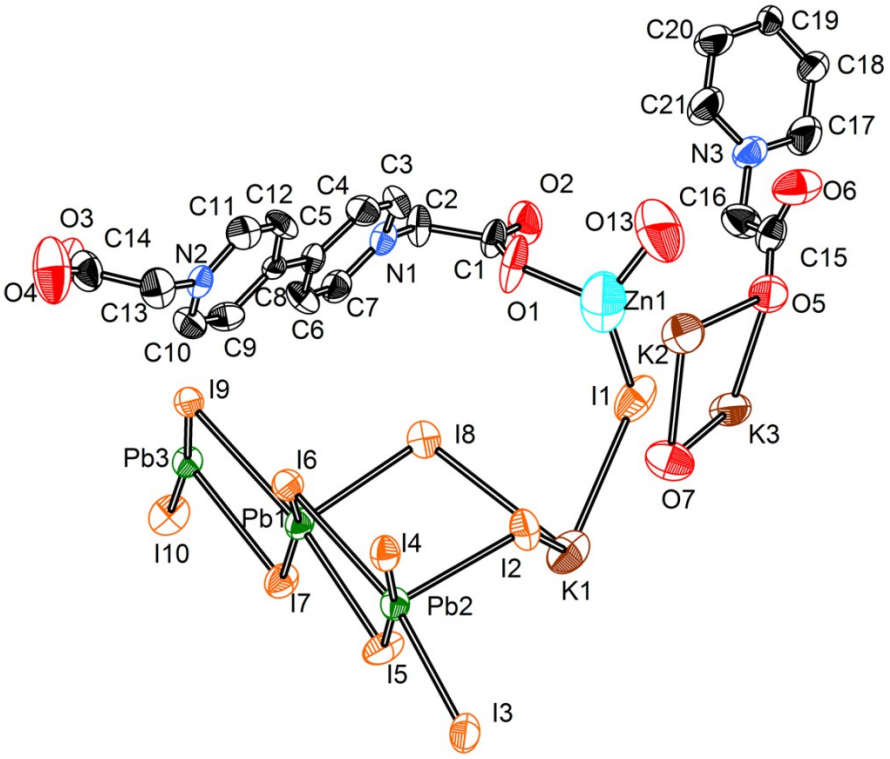

Figure S1. Asymmetric unit of **1** (50% probability ellipsoids level)

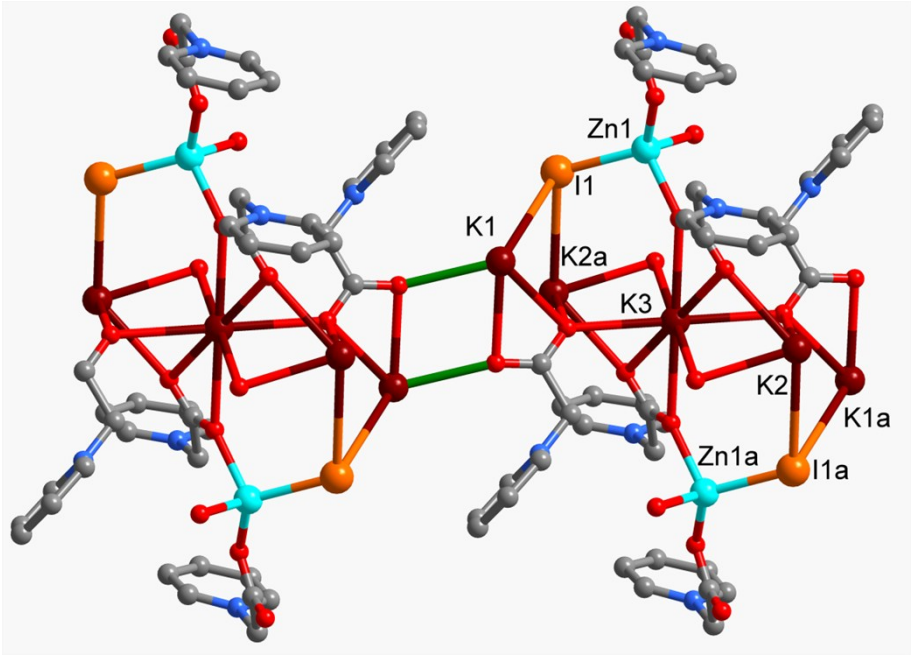

Figure S2. The $K_5Zn_2O_{13}I_2$ clusters in the zigzag K-Zn-O ribbon

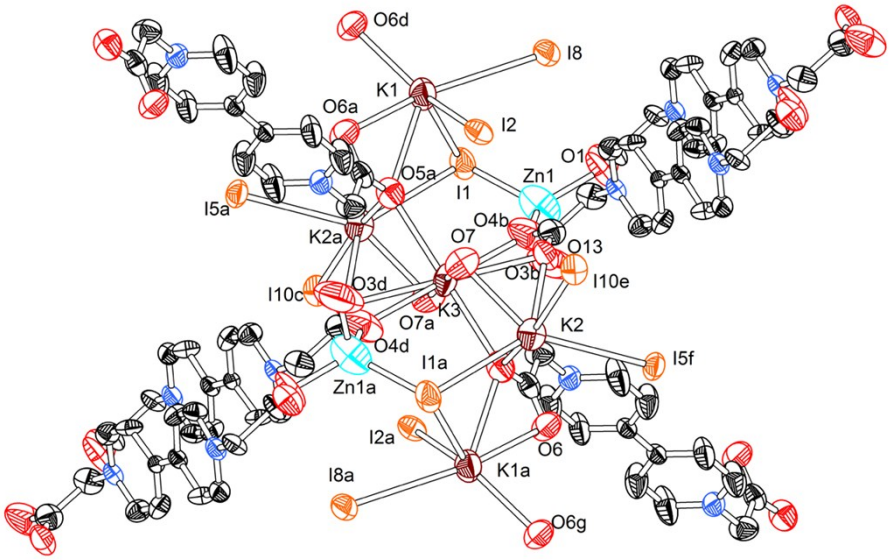

Figure S3. The coordination environment of the K and Zn atoms in **1**, showing the atom-labelling scheme and 50% probability displacement ellipsoids [Symmetry codes: (a) 2-x, 1-y, -z; (b) 2-x, 1-y, 1-z; (c) 1-x, -y, -z; (d) x, -1+y, z; (e) 1+x, 1+y, z; (f) x, 1+y, z; (g) 2-x, 2-y, -z]

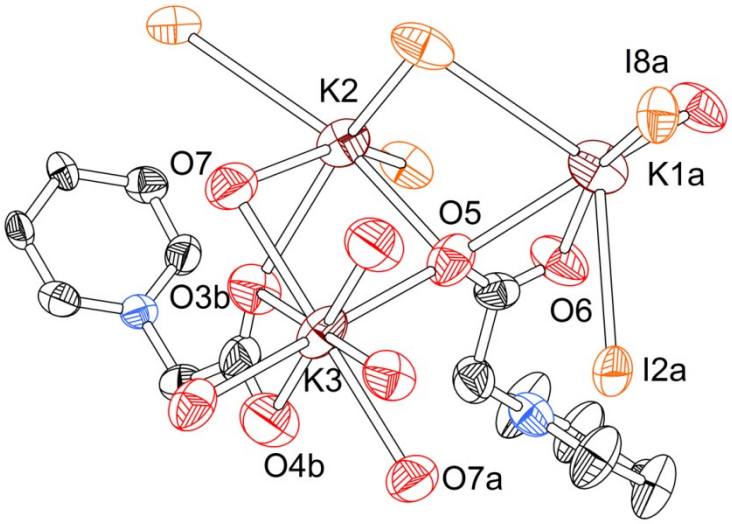

Figure S4. The K atoms interconnection through the O atoms in **1** [Symmetry codes: (a) 2-x, 1-y, -z; (b) 2-x, 1-y, 1-z]

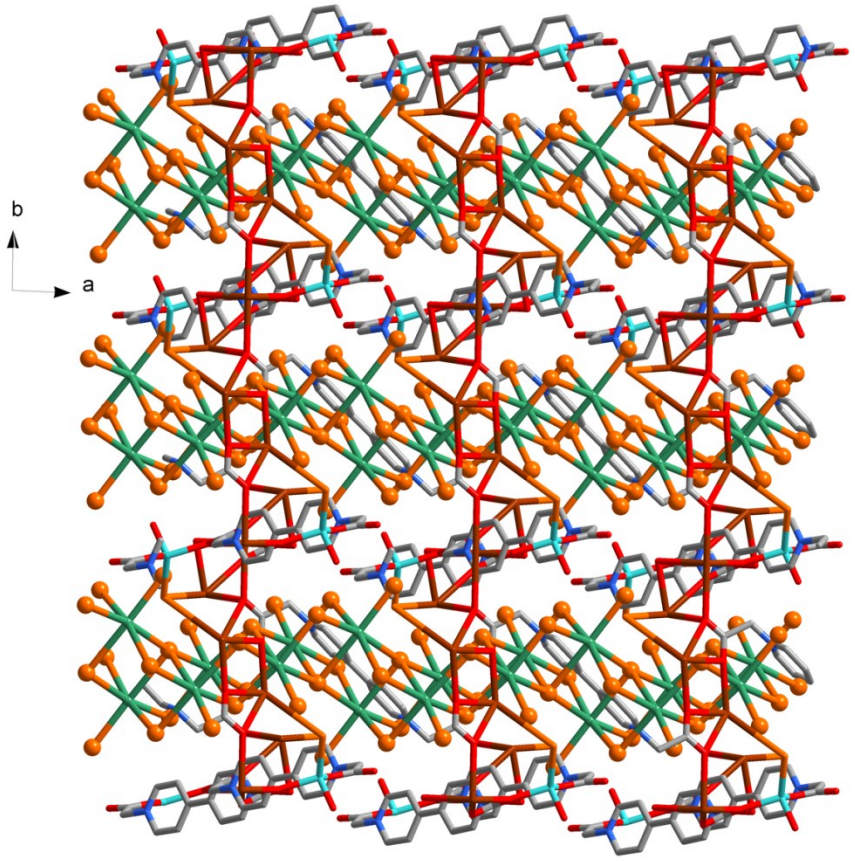

Figure S5. Crystal packing of **1** along the c axis; Hydrogen atoms are omitted for clarity.

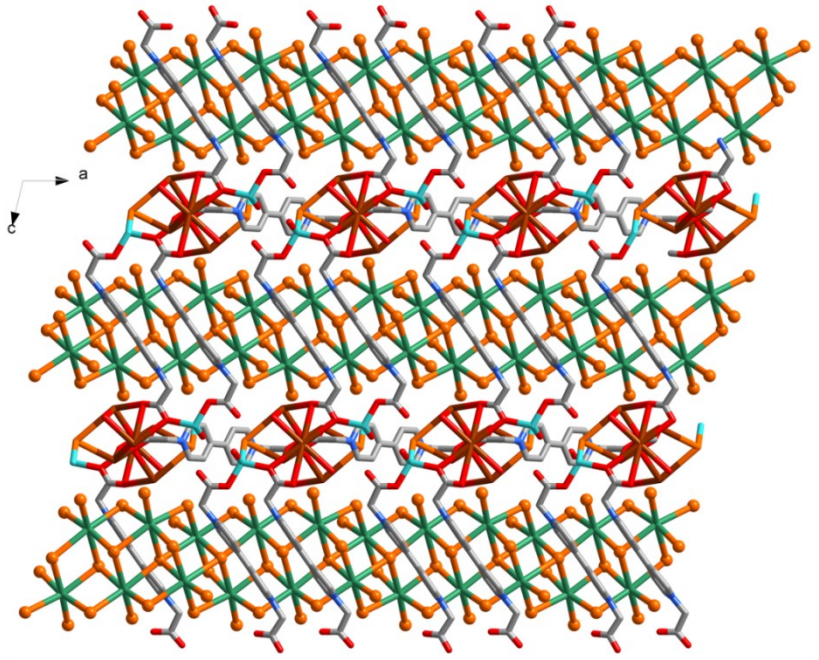

Figure S6. Crystal packing of **1** along the b axis; Hydrogen atoms are omitted for clarity.

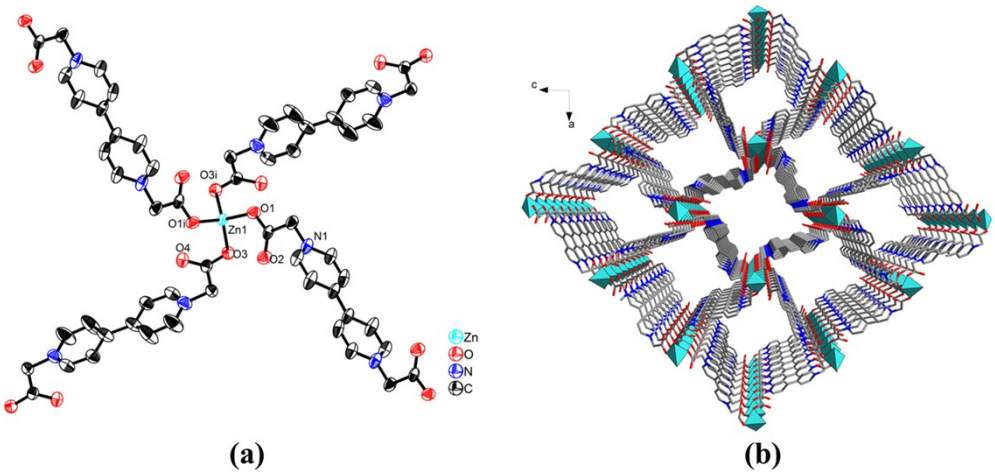

Figure S7. The crystal structure of **2** (a) and its packing along b axis; H atoms and iodide anions are omitted for clarity.

3. X-ray powder diffraction analysis

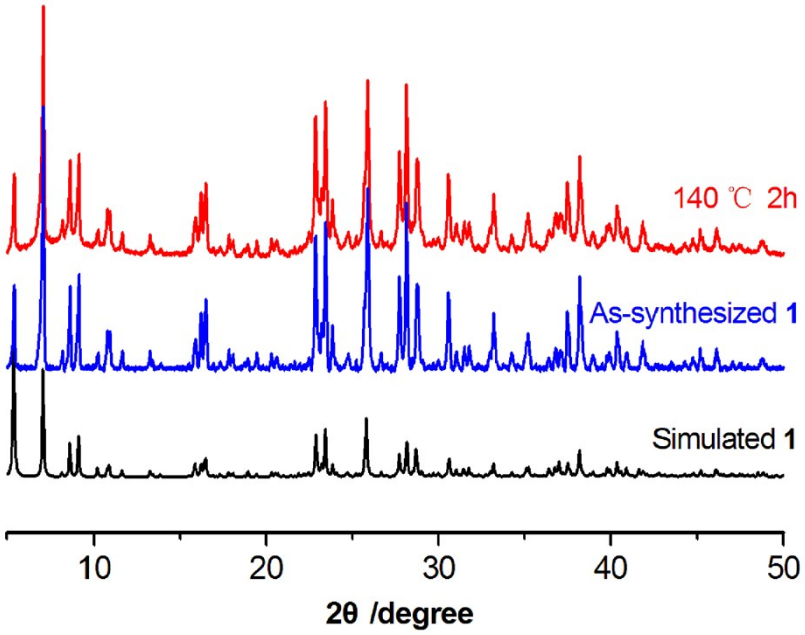

Figure S8. Variable-temperature PXRD patterns of hybrid **1**

4. Infrared spectral analysis

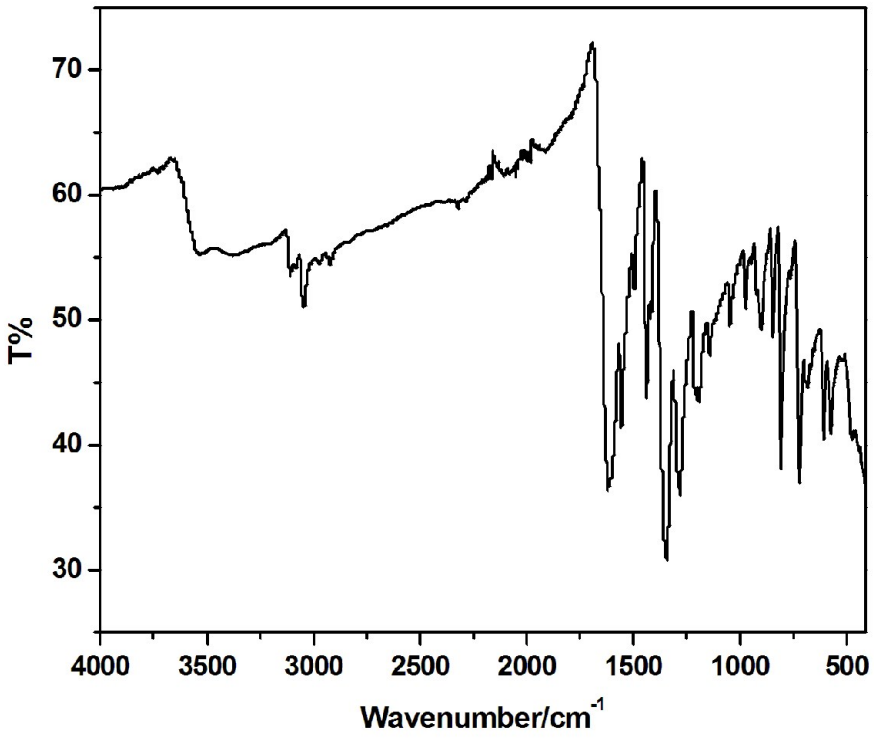

Figure S9. Infrared spectrum of hybrid **1**

5. Thermo-gravimetric analysis (TGA)

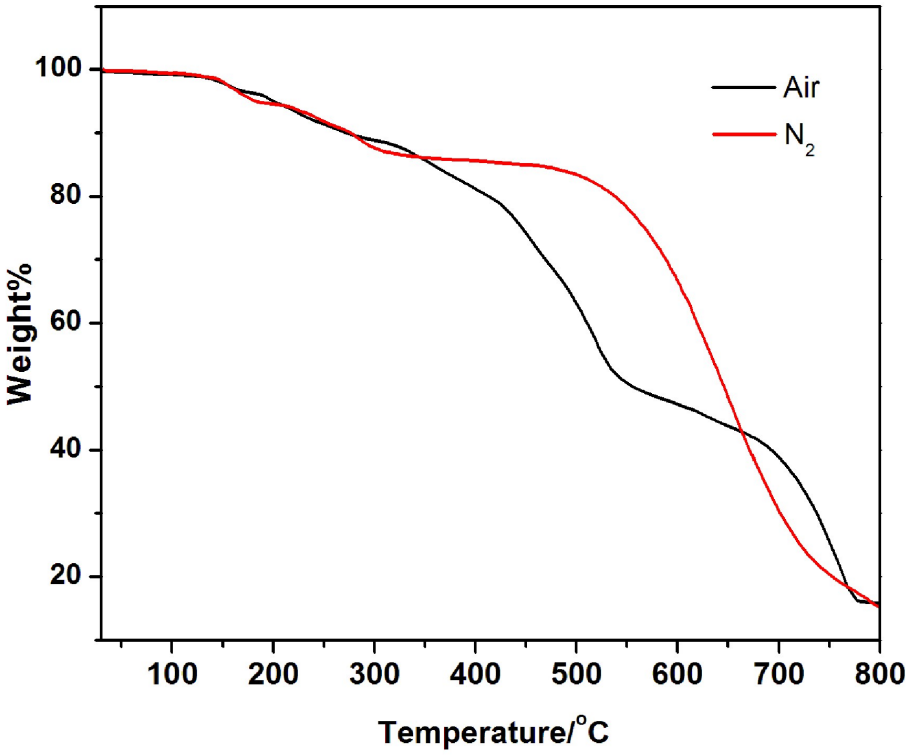

Figure S10. TGA curve of **1** under N_2 and air atmosphere with a heating rate of 10 °C/min

6. Theoretical calculations

The crystal structure optimization of **1** is performed using plane-wave pseudo potential method as implemented in CASTEP code.[S3-S4] The exchange and correlation interactions were modeled by using the generalized-gradient approximation developed by Perdew, Burke, and Ernzerhof (GGA-PBE).[S5] The cut-off energy for the plane wave expansion was set to 820 eV and a Monkhorst-Pack k-point mesh for the Brillouin-zone integration was generated with 2 × 2 × 2. The optimized crystal structures are consistent with the experimental data. It is well-know that the standard density functional theory (DFT) methods, such as the Perdew-Burke-Ernzerhof (PBE) functional, contains unphysical self-Coulomb repulsion, leading to a systematic underestimate of band gaps.[S6] For the improvement of the band gap, Tran-Blaha modified Becke-Johnson (mBJ) potential[S7-S8] is as efficient as other hybrid functional.[S9-S10] It is an orbital independent exchange correlation potential with semilocal approximation and a screening effect. The mBJ allows the calculation of electronic band structure with accuracy close to the very expensive GW calculations. So, in this work, the electronic structure of **1** was calculated by the full-potential linearized augmented plane-wave (LAPW) method as implemented in the WIEN2k code.[S11] Then the mBJ potential was adopted in our calculations. The spin-orbital coupling (SOC) effect was also considered for all the atoms. And the calculated band structure of **1** and its total and partial DOS are shown as Figure S11-S12.

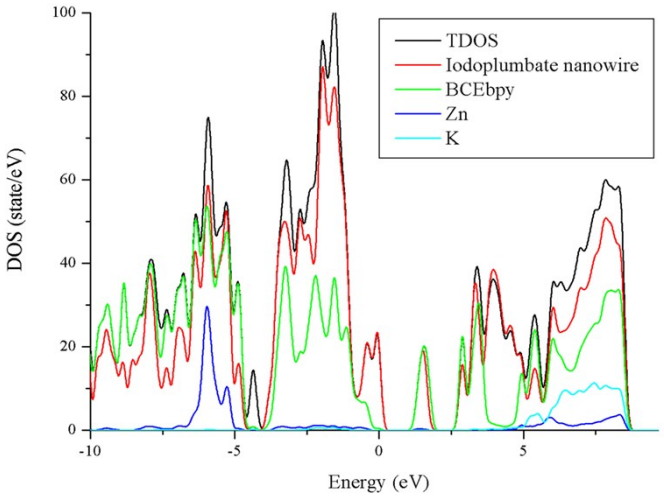

Figure S11. Total and partial DOS of **1**. The Fermi level is chosen as the energy reference at 0 eV.

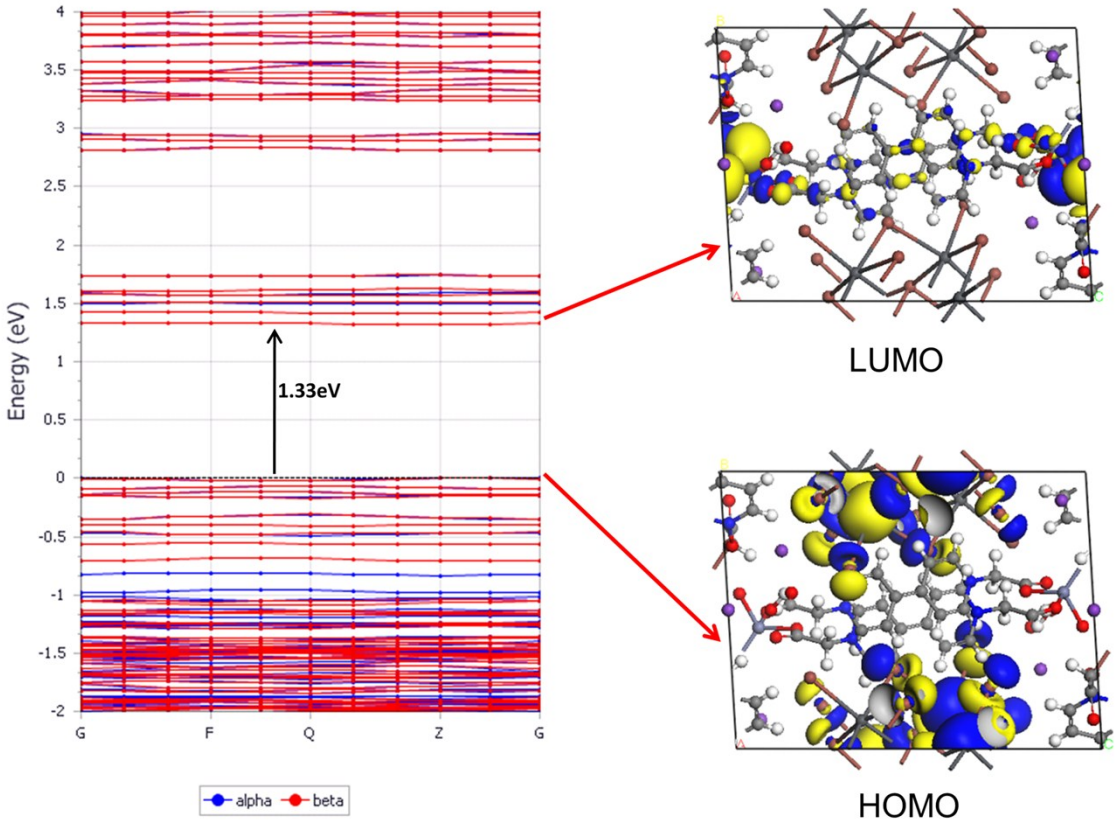

Figure S12. Calculated band structure of **1**.

7. Reversible photoconductivity cycle measures

Figure S13. Photograph of hybrid **1**

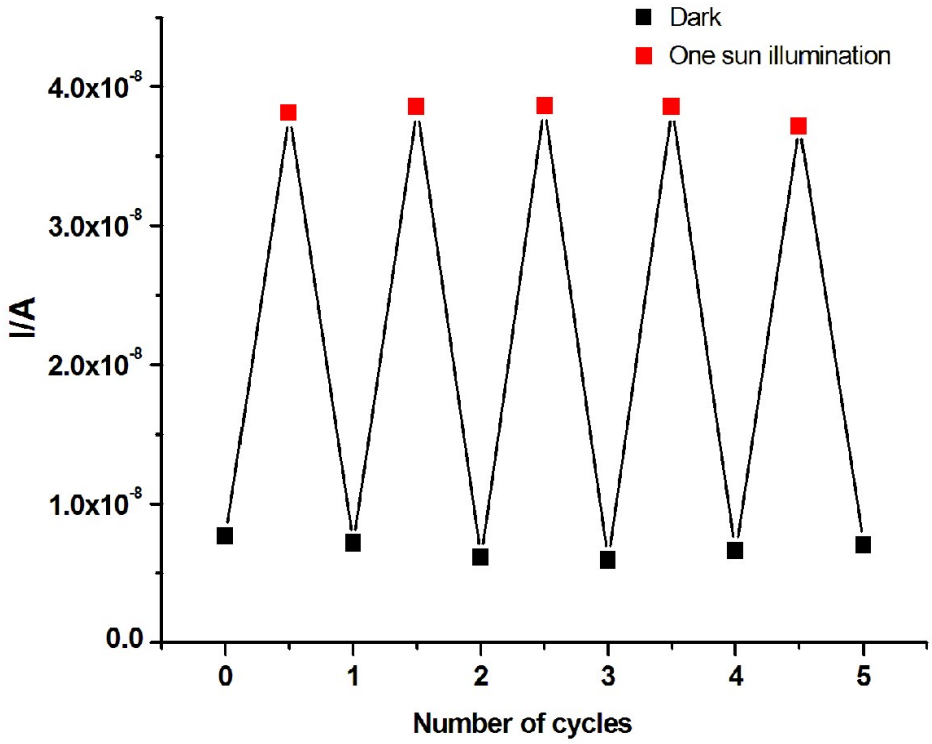

Figure S14. Modulation of the current at 5V due to alternating sun illumination and dark treatment

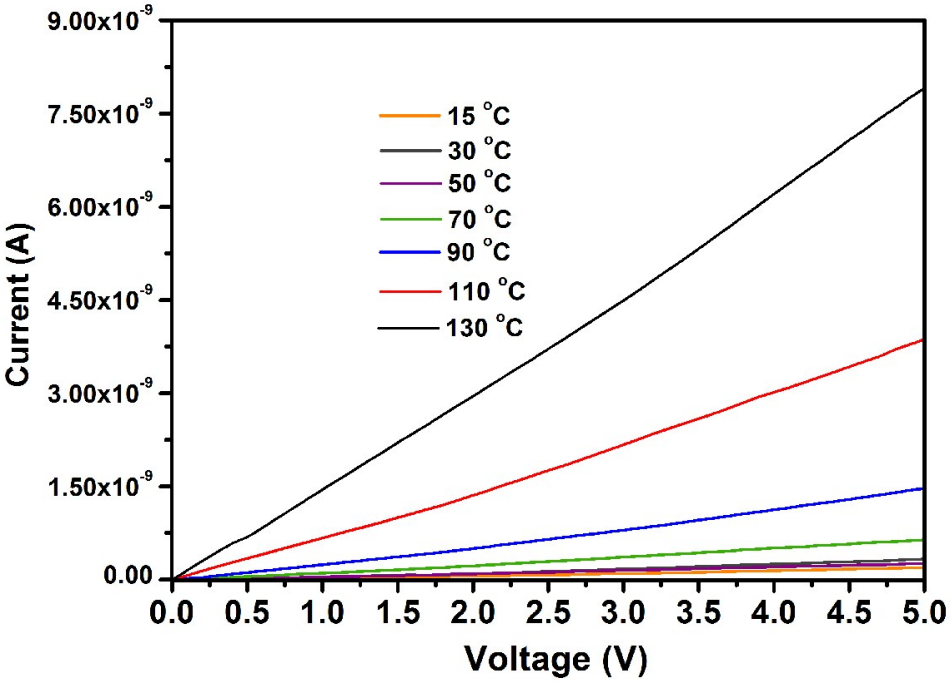

Figure S15. Variable temperature I-V curves of **2**.

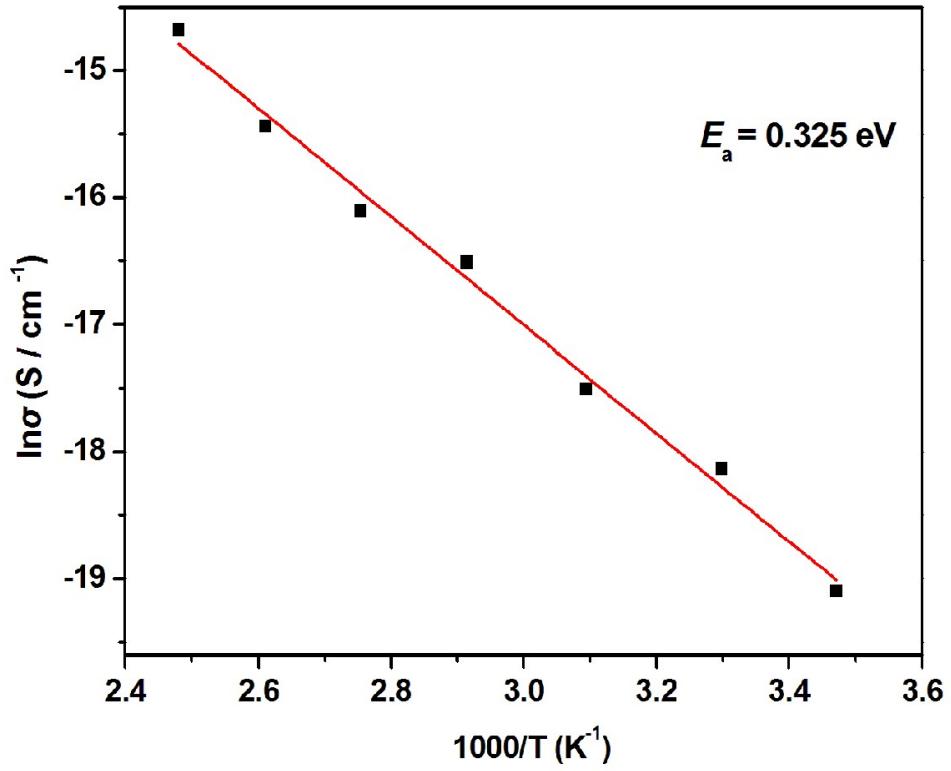

Figure S16. Arrhenius plots of **2**, Ea is the activation energy for the conduction.

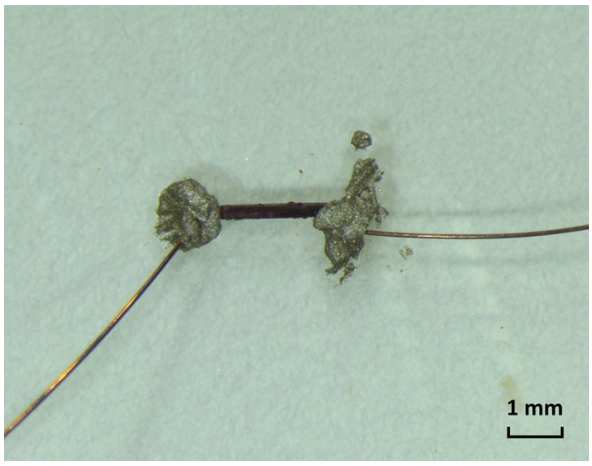

Figure S17. Photograph of a two probe device made from a single crystal of 1 using the gold wire paste approach.

8. References

[S1] A. D. Phillips, Z. Fei, W. H. Ang, R. Scopelliti, P. J. Dyson, *Cryst. Growth Des.* **2009**, *9*, 1966.

[S2] Sheldrick. G., *Acta Cryst.* **2008**, *A64*, 112.

[S3] S. J. Clark, M. D. Segall, C. J. Pickard, P. J. Hasnip, M. I. J. Probert, K. Refson, M. C. Payne, *Z. Kristallogr.*, **2005**, *220*, 567.

[S4] M. D. Segall, P. J. D. Lindan, M. J. Probert, C. J. Pickard, P. J. Hasnip, S. J. Clark, M. C. Payne, *J. Phys.: Condens. Matter*, **2002**, *14*, 2717.

[S5] J. P. Perdew, K. Burke, M. Ernzerhof, *Phys. Rev. Lett.*, **1996**, *77*, 3865.

[S6] P. Mori-Sánchez, A. J. Cohen, W. Yang, *Phys. Rev. Lett.*, **2008**, *100*, 146401.

[S7] F. Tran, P. Blaha, *Phys. Rev. Lett.*, **2009**, *102*, 226401

[S8] D. Koller, F. Tran, P. Blaha, *Phys. Rev. B*, **2012**, *85*, 155109

[S9] H. Kino, F. Aryasetiawan, I. Solovyev, T. Miyake, T. Ohno, K. Terakura, *Phys. B: Condens. Matter*, **2003**, *329*, 858.

[S10] S. Chettri, D. P. Rai, A. Shankar, R. Khenata, M. P. Ghimire, R. K. Thapa, S. B. Omran, *Int. J. Mod. Phys. B*, **2016**, *30*, 1650078

[S11] P. Blaha, K. Schwarz, G. Madsen, D. Kvasnicka, Wien2k Package.